Effects of mechanical stress on electromigration-driven transgranular void dynamics in passivated metallic thin films

M. Rauf Gungor and Dimitrios Maroudas[a)]
Department of Chemical Engineering, University of California, Santa Barbara, California 93106-5080

Leonard J. Gray
Computer Sciences and Mathematics Division, Oak Ridge National Laboratory, Oak Ridge, Tennessee 37831

(Received 21 September 1998; accepted for publication 21 October 1998)

The combined effects of mechanical stress and surface electromigration on the dynamics of transgranular voids in passivated metallic thin films are analyzed based on self-consistent dynamical simulations. Depending on the strength of the electric and stress fields, void morphological instabilities can lead to film failure by propagation from the void surface of either faceted slits or finer-scale crack-like features. Most importantly, there exists a narrow range of applied stress for given strength of electric field over which slit formation can be inhibited completely. © *1998 American Institute of Physics.* [S0003-6951(98)00352-0]

The reliability of integrated circuits is limited by the failure of polycrystalline aluminum and copper thin films, which are used for device interconnections.[1] The widths of these films have decreased to submicron scale toward ultralarge-scale integration (ULSI). Failure mechanisms in these systems are driven mainly by electromigration. In films that are mechanically confined due to their encapsulation by a passivation material, thermomechanical stresses are induced during film cooling after passivation. Voids may nucleate at the film edges as a mechanism of stress relaxation. After cooling and aging, the films are in a state of hydrostatic tension;[1,2] this residual stress can drive significant void morphological evolution that may cause failure. It has been established experimentally that transgranular voids are common sources of failure in bamboo films, where grain boundaries are almost perpendicular to the length direction of the film;[3,4] such voids are not intersected by grain boundaries. In spite of recent theoretical studies of electromigration-induced transgranular void dynamics[5–10] and our understanding of surface instabilities in mechanically stressed solids,[11] the combined effects of electromigration and mechanical stress on void morphological evolution and interconnect failure are not very well understood.

The purpose of this letter is to examine theoretically the effects of the simultaneous action of applied mechanical stress and electric field on transgranular void dynamics. Based on self-consistent simulations of void morphological evolution, failure is predicted to occur by the coupling of two modes of surface morphological instability; one that is current driven and another that is stress driven. The void surface morphology associated with these instabilities consists of faceted slits and crack-like features, respectively, and is consistent with recent experimental observations.[4] Most importantly, it is predicted that appropriate tailoring of the current and stress conditions can stabilize the void surface, thus inhibiting failure.

Our analysis is based on a continuum formalism of surface mass transport under the action of external fields.[7,10] The total mass flux, $\mathbf{J}_s$, on the void surface is given by

$$\mathbf{J}_s = -D_s \delta_s / \Omega k_B T (q_s^* \mathbf{E}_s + \nabla_s \mu), \tag{1}$$

where D_s is the surface atomic diffusivity, Ω is the atomic volume, δ_s/Ω is the number of surface atoms per unit area, k_B is Boltzmann's constant, T is temperature, q_s^* is a surface effective charge,[1] $\mathbf{E}_s$ is the local electric field component tangent to the void surface, μ is the chemical potential of an atom on the void surface, and ∇_s is the surface gradient operator. Both surface free energy and elastic strain energy contribute to μ, which is expressed by

$$\mu = \mu_0 + \Omega[\tfrac{1}{2}\,\mathrm{tr}(\boldsymbol{\sigma}\cdot\boldsymbol{\epsilon}) - \gamma\kappa]. \tag{2}$$

In Eq. (2), μ_0 is a reference chemical potential for a flat stress-free surface, $\boldsymbol{\sigma}$ and $\boldsymbol{\epsilon}$ are the local stress and strain tensors, respectively, γ is the surface free energy per unit area, and κ is the local surface curvature. Mass conservation gives the evolution of the local displacement normal to the void surface, u_n, through the continuity equation, i.e.,

$$\frac{\partial u_n}{\partial t} = -\Omega \nabla_s \cdot \mathbf{J}_s. \tag{3}$$

The electric field, $\mathbf{E}$, in the metallic conductor can be written as $\mathbf{E} \equiv -\boldsymbol{\nabla}\cdot\boldsymbol{\Phi}$, where the electrostatic potential, Φ, obeys Laplace's equation, i.e., $\nabla^2\Phi = 0$. Cauchy's mechanical equilibrium equation, $\nabla\sigma = \mathbf{0}$, also is satisfied. The mechanical deformation of the solid is addressed within the framework of isotropic linear elasticity and in the limit of infinitesimal displacement: $\boldsymbol{\epsilon} = (1/2)[\nabla\mathbf{u} + (\nabla\mathbf{u})^T]$, where $\mathbf{u}$ is the displacement field and ^{T} denotes the transpose of a tensor. Our analysis is limited in two dimensions, x (length) and y (width), which implies that the void extends throughout the film thickness (in z).[10,12] In this two-dimensional (2D) model, plane strain conditions are assumed. The void surface is considered to be traction free, while the boundaries of the 2D computational domain are subject to a constant applied stress, σ_0, imposed as hydrostatic tension. This loading resembles the strain state of interconnect films after thermal processing and aging. The void surface and the film's edges are modeled as electrically insulating boundaries,

a)Electronic mail: dimitris@calypso.ucsb.edu

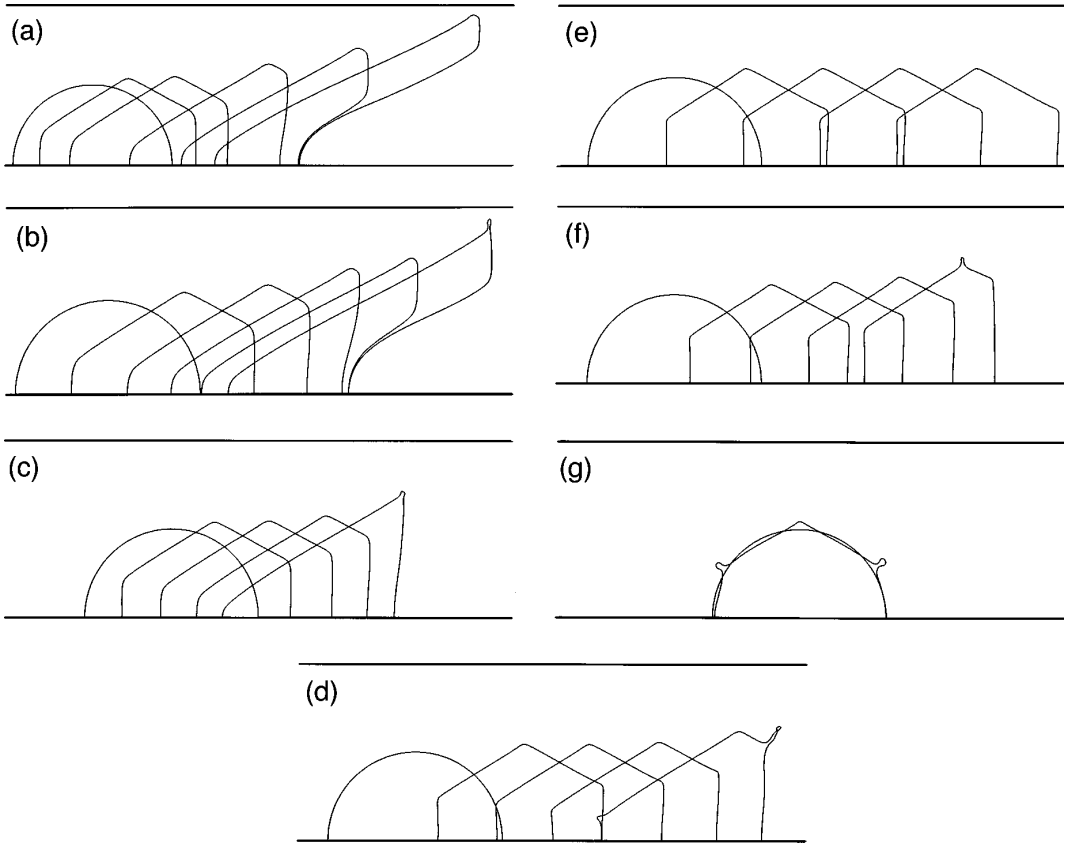

FIG. 1. Evolution of transgranular voids in a ⟨111⟩-oriented grain of a metallic film under the action of an electric field directed from left to right. The corresponding parameters are $\Gamma=150$, $\Lambda=0.5$, $A=10$, $m=3$, $\phi=-15°$, and (a) $\Sigma=0$, (b) $\Sigma=0.3$, (c) $\Sigma=0.7$, (d) $\Sigma=1.05$, (e) $\Sigma=1.075$, (f) $\Sigma=1.1$, and (g) $\Sigma=1.5$. The times corresponding to the different morphologies from left to right are: (a) $t=0$, 0.574, 1.272, 2.486, 3.395, $3.929\times10^{-4}\tau$; (b) $t=0$, 1.047, 2.061, 2.776, 3.228, $3.608\times10^{-4}\tau$; (c) $t=0$, 0.672, 1.453, 2.176, $2.773\times10^{-4}\tau$; (d) $t=0$, 1.901, 2.974, 4.012, $4.959\times10^{-4}\tau$; (e) $t=0$, 1.314, 2.702, 4.089, $5.477\times10^{-4}\tau$; (f) $t=0$, 1.778, 2.882, 3.976, $5.125\times10^{-4}\tau$; and (g) $t=0$, $2.041\times10^{-6}\tau$.

while a constant electric field, $\mathbf{E}_\infty=E_\infty\hat{\mathbf{x}}$, is imposed far away from the void. Surface adatom diffusivity is expressed by $D_s=D_{s,\min}f(\theta)$, where $D_{s,\min}$ is the minimum surface diffusivity corresponding to a specific surface orientation, and $f(\theta)\geqslant1$ is an anisotropy function of the angle θ formed by the local tangent to the surface and $\mathbf{E}_\infty$. In the present treatment, we have adopted the simple functional form $f(\theta)=1+A\cos^2[m(\theta+\phi)]$, where A, m, and ϕ are dimensionless parameters that determine the strength of the anisotropy, the grain symmetry, and the misorientation of a symmetry direction of fast surface diffusion with respect to the applied electric field, respectively. On the other hand, γ is assumed to be isotropic in Eq. (2); this assumption is justified by recent atomistic simulations, according to which the dependence of γ on θ is weaker by orders of magnitude than that of D_s.[13] Additional mass transport modeling assumptions have been discussed in Refs. 10 and 12.

Dimensional analysis of Eqs. (1)–(3) yields three important dimensionless parameters: the *surface electrotransport number*,[7] $\Gamma\equiv E_\infty q_s^* w^2/(\gamma\Omega)$, the scaled strain energy, $\Sigma\equiv\sigma_0^2 w/(E\gamma)$, and the dimensionless void size, $\Lambda\equiv w_t/w$. Γ scales electric forces with capillary forces and Σ scales elastic strain energy with surface energy; E is the Young's modulus of the material, w is the width of the film, and w_t is the initial extent of the void across the film. The resulting time scale is $\tau\equiv k_BTw^4/(D_{s,\min}\delta_s\gamma\Omega)$. In an Al film of $w\approx1$ μm, $\Gamma=50$ corresponds to a current density of about 2 MA/cm^2, which is typical of accelerated electromigration experiments.[3,4] For the same film, $\Sigma=1$ corresponds to a stress of about 140 MPa; this is typical of residual stresses in interconnect lines after cooling and aging.[1,2] Finally, for the same film τ is estimated on the order of 10^4 h.

The electric field and the stress tensor on the domain boundary are computed using the Galerkin Boundary Element formulation of Ref. 14. The surface flux divergence is calculated based on a centered finite-difference scheme and Eq. (3) is integrated using an Adams–Bashforth algorithm. In the simulations, the initial void shape is taken to be semicircular, i.e., a configuration that includes all possible surface orientations with respect to $\mathbf{E}_\infty$.

Void dynamical behavior at constant void volume is analyzed parametrically in a six-dimensional (6D) hyperspace defined by the parameters Γ, Σ, Λ, A, m, and ϕ. Here, we select sixfold grain symmetry, $m=3$, which is characteristic of ⟨111⟩-oriented grains that are common in textured interconnect lines. We focus on a point in parameter space that corresponds to electromigration-induced slit-like failure, as shown in Fig. 1(a); this is given by $\Gamma=150$, $\Lambda=0.5$, $A=10$, $\phi=-15°$, $\Sigma=0$ and represents our reference point for parametric study in Σ. Under the above conditions, the void surface becomes faceted initially assuming a semihexagonal shape. This is followed by a facet selection process, where two facets elongate at the expense of the facet that lies between them. Facet selection proceeds by elimination of this facet leading to a wedge-shaped void, which is destabilized further to give a slit-like shape with two parallel facets; the

slit becomes narrower and propagates in the direction of these parallel facets causing failure. Such slit formation is the result of an instability in the competition for mass transport between electromigration and capillarity.

Figures 1(b)–1(g) demonstrate how the dynamical response of the void changes as the applied stress increases from the point that corresponds to the dynamical behavior of Fig. 1(a). In Fig. 1(b), $\Sigma = 0.3$, and the dynamical sequence resembles closely that of Fig. 1(a): faceting is followed by facet selection, wedge formation, and faceted slit formation and propagation. In this case, however, after the slit propagates a certain distance, a finer-scale crack-like feature forms and its tip propagates at a speed greater by about two orders of magnitude than the average void migration speed. Thus, open-circuit failure is caused by the fast propagation of the crack-like feature's tip; this feature is narrower by at least an order of magnitude than the original slit. Figure 1(c) shows the corresponding dynamical sequence at $\Sigma = 0.7$. The void shape evolves again into a wedge but, interestingly, subsequent faceted slit formation is not observed in this case. Instead, a fine-scale crack-like feature forms at the tip of the wedge and propagates fast to cause failure. As Σ keeps increasing, not even the facet selection process can be completed toward wedge formation. Instead, crack-like features appear at corners of the faceted void shape, where the strain energy density increases abruptly. Such a dynamical behavior is shown in Fig. 1(d) at $\Sigma = 1.05$; again, failure occurs by tip propagation of the crack-like feature.

The dynamical behavior of the transgranular void changes drastically if the applied stress is increased slightly to $\Sigma = 1.075$, as demonstrated in Fig. 1(e). Specifically, within the interval $1.05 < \Sigma < 1.1$, neither electromigration-induced facet selection nor stress-induced crack formation are initiated. Instead, the faceted void is stable and migrates along the film at constant speed maintaining its semihexagonal shape. This response implies that film failure due to electromigration-induced slit-like morphological instabilities of the void surface can be inhibited by the action of a mechanical stress. The applied stress level must be just enough to balance the destablizing effect of the electric field without causing crack-like morphological instabilities that lead to a faster mode of failure. This theoretical prediction is made for the first time based on self-consistent simulation.

Increasing the applied stress above the narrow range of stability leads to formation of crack-like features that emanate from the faceted void surface. This is shown in Fig. 1(f) for $\Sigma = 1.1$. Facet selection can be initiated again as in the case of Fig. 1(d); however, the strain energy distribution on the void surface is different here and leads to formation of a crack-like feature at the top of the void surface. At higher levels of applied stress, crack-like failure can occur even faster than facet selection. This is demonstrated in Fig. 1(g) for $\Sigma = 1.5$; crack-like features form symetrically at the two corners of the faceted shape where the strain energy density along the void surface increases most abruptly.

The predicted general mixed mode of failure, where the void surface exhibits electromigration-induced features, such as faceted slits, coexisting with stress-induced crack-like features is consistent with recent experimental observations. For example, such void morphologies have been observed by Joo and Thompson through SEM measurements in passivated, single-crystalline Al films.[4] Generally, the location of crack formation is correlated strongly with the distribution of elastic strain energy on the faceted void surface.

In conclusion, self-consistent numerical simulations have been developed to investigate the simultaneous effects of applied mechanical stresses and electric fields on transgranular void dynamics and the resulting failure mechanisms in passivated metallic thin films. Under such conditions, failure occurs through the coupling of two modes of void morphological instability: one is driven by electromigration and leads to facet selection and faceted slit formation, while the other is driven by stress and leads to formation of finer-scale crack-like features. Most interestingly, there exists a narrow range of electromechanical conditions over which the effects of the two driving forces can be balanced by the stabilizing effect of capillary forces; therefore, the faceted void surface becomes stable and failure is prevented. This possibility has very important implications for the reliability of metallic thin-film interconnects: thermal processing strategies of these films can be developed in order to tailor the resulting state and level of stress in the films to inhibit electromigration-induced failure. (The length scale characteristic of the width of the crack-like features predicted by our simulations is on the order of nanometers, i.e., very fine for phenomenological analysis. Molecular-dynamics simulations of stress-driven void tip phenomena are underway to elucidate the possible role of dislocation-mediated mechanisms and upgrade the present mesoscopic modeling accordingly.)

The authors acknowledge fruitful discussions with C. V. Thompson, S. J. Zhou, and D. R. Clarke. This work was supported by the Frontiers of Materials Science Program of the UCSB Materials Research Laboratory and Los Alamos National Laboratory (Award No. STB-UC:97-63), by NSF through a CAREER Award to DM (ECS-95-01111) by ORISE and the U.S. DOE under Contract No. DE-AC05-96OR22464 with Lockheed Martin Energy Research Corporation.

[1] P. S. Ho and T. Kwok, Rep. Prog. Phys. **52**, 301 (1989); C. V. Thompson and J. R. Lloyd, MRS Bull. **18**, 19 (1993), and references therein.
[2] See, e.g., A. I. Sauter and W. D. Nix, J. Mater. Res. **7**, 1133 (1992).
[3] J. E. Sanchez, Jr., L. T. McKnelly, and J. W. Morris, Jr., J. Electron. Mater. **19**, 1213 (1990); J. Appl. Phys. **72**, 3201 (1992); J. H. Rose, Appl. Phys. Lett. **61**, 2170 (1992); O. Kraft, S. Bader, J. E. Sanchez, Jr., and E. Arzt, Mater. Res. Soc. Symp. Proc. **309**, 199 (1993); E. Arzt, O. Kraft, W. D. Nix, and J. E. Sanchez, Jr., J. Appl. Phys. **76**, 1563 (1994).
[4] Y.-C. Joo and C. V. Thompson, J. Appl. Phys. **81**, 6062 (1997).
[5] Z. Suo, W. Wang, and M. Yang, Appl. Phys. Lett. **64**, 1944 (1994); W. Q. Wang, Z. Suo, and T.-H. Hao, J. Appl. Phys. **79**, 2394 (1996).
[6] O. Kraft and E. Arzt, Appl. Phys. Lett. **66**, 2063 (1995); O. Kraft and E. Arzt, Acta Mater. **45**, 1599 (1997).
[7] D. Maroudas, Appl. Phys. Lett. **67**, 798 (1995); D. Maroudas, M. N. Enmark, C. M. Leibig, and S. T. Pantelides, J. Comp.-Aided Mater. Des. **2**, 231 (1995).
[8] L. Xia, A. F. Bower, Z. Suo, and C. F. Shih, J. Mech. Phys. Solids **45**, 1473 (1997).
[9] M. Schimschak and J. Krug, Phys. Rev. Lett. **80**, 1674 (1998).
[10] M. R. Gungor and D. Maroudas, Appl. Phys. Lett. **72**, 3452 (1998).
[11] See, e.g., D. J. Srolovitz, Acta Metall. **37**, 621 (1989); W. H. Yang and D. J. Srolovitz, Phys. Rev. Lett. **71**, 1593 (1993).
[12] M. R. Gungor and D. Maroudas, Surf. Sci. **418**, L1055 (1998).
[13] C.-L. Liu, J. M. Cohen, J. B. Adams, and A. F. Voter, Surf. Sci. **253**, 334 (1991).
[14] L. J. Gray, D. Maroudas, and M. N. Enmark, Comp. Mech. **22**, 187 (1998).